Using Remote Sensing Images to Design Optimal Field Sampling Schemes

P. Debba[1]

[1] CSIR, Logistics and Quantitative Methods, CSIR Built Environment

Outline

1. Introduction
2. Optimized sampling schemes case studies
   - Optimized field sampling representing the overall distribution of a particular mineral
   - Deriving optimal exploration target zones

IMPORTANCE OF OPTIMAL SAMPLING SCHEMES

- Sample - small subset of the population of interest.
- Sample should represent the characteristics of the population (parameters / distribution).
- Environmental studies:
  - where to sample?
  - what to sample?
  - and how many samples to obtain?
- Remote sensing as ancillary information in the design of optimal sampling schemes.
- Advantages of using remote sensing images:
  - Provides a synoptic overview of a large area
  - Wealth of information over the entire area
  - In these methods sampling avoids subjective judgement
  - Reduces costs and saves time on the field (fewer samples)

OVERVIEW OF HYPERSPECTRAL REMOTE SENSING

Hyperspectral sensors

- record the reflectance in many narrow contiguous bands
- various parts of the electromagnetic spectrum (visible - near infrared - short wave infrared)
- at each part of the electromagnetic spectrum results in an image

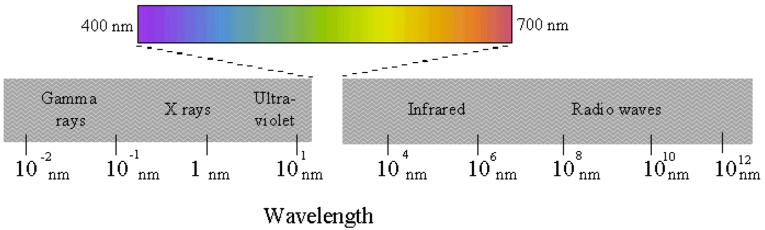

Figure: Spectral Range

OVERVIEW OF HYPERSPECTRAL REMOTE SENSING (cont. . .)

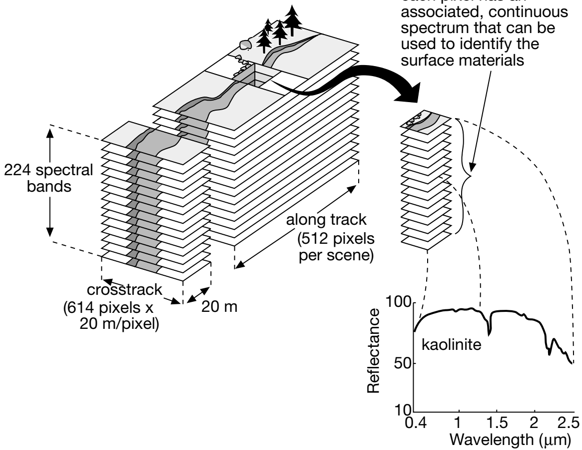

Figure: Hyperspectral cube

OVERVIEW OF HYPERSPECTRAL REMOTE SENSING (cont. . .)

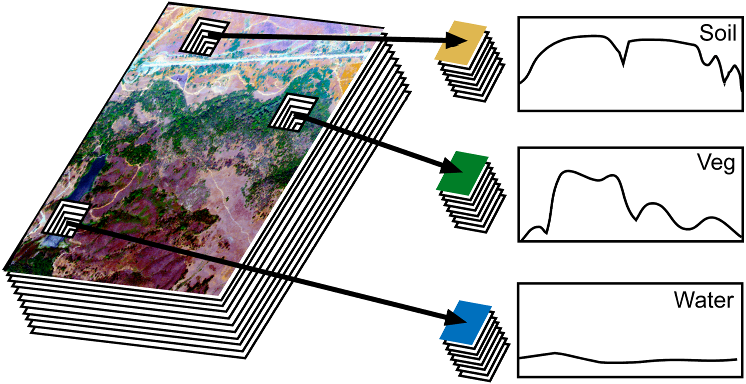

Figure: Pixels in hyperspectral image

OVERVIEW OF HYPERSPECTRAL REMOTE SENSING (cont. . .)

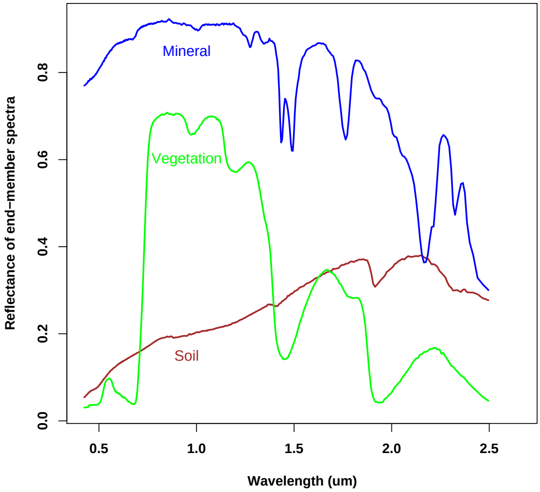

Figure: Example of 3 different spectral signatures

Outline

1. Introduction
2. Optimized sampling schemes case studies
   - Optimized field sampling representing the overall distribution of a particular mineral
   - Deriving optimal exploration target zones

OBJECTIVE OF STUDY

Using a hyperspectral image, to guide field sampling collection to those pixels with the highest likelihood for occurrence of a particular mineral, for example alunite, while representing the overall distribution of alunite.

Usefulness: To create a mineral alteration map

STUDY SITE

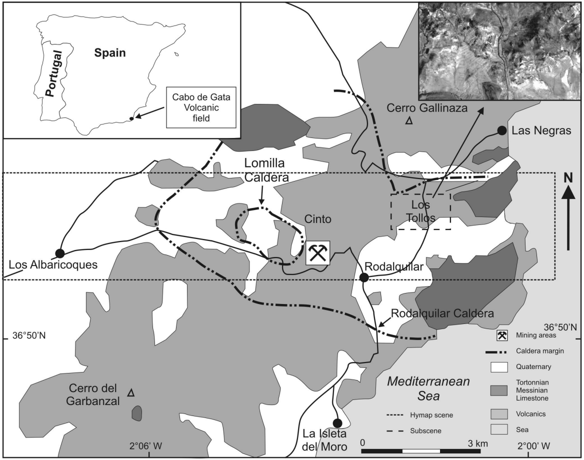

Figure: A generalized geological map of the Rodalquilar study area showing the flight line and the hyperspectral data

DATA USED

- HyMap: 126 bands – 0.4–2.5 μm
- Geology: 30 bands – 1.95–2.48 μm
- Distinctive absorption features at wavelengths near 2.2 μm
- We collected field spectra during the over-flight using the Analytical Spectral Device (ASD) fieldspec-pro spectrometer – 0.35–2.50 μm

ENDMEMBER SPECTRA

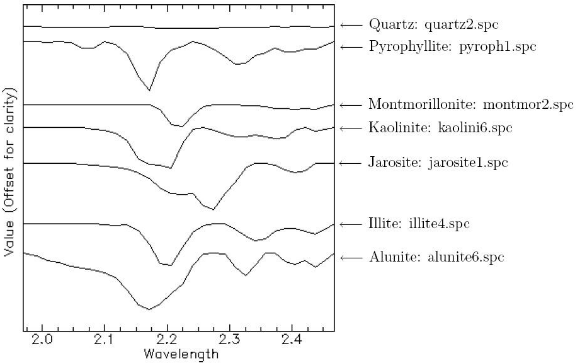

Figure: Plot of 7 endmembers from USGS spectral library for the 30 selected bands, enhanced by continuum removal.

CONTINUUM REMOVAL

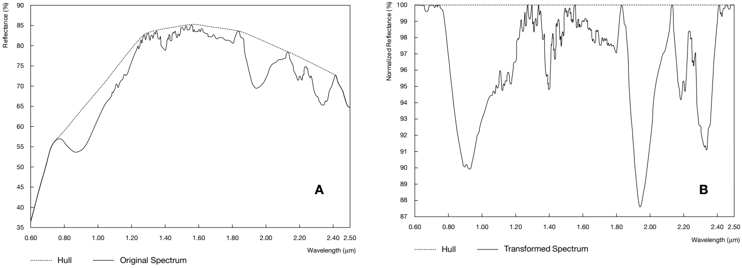

Figure: Concept of the convex hull transform; (A) a hull fitted over the original spectrum; (B) the transformed spectrum.

CONTINUUM REMOVAL (cont. . .)

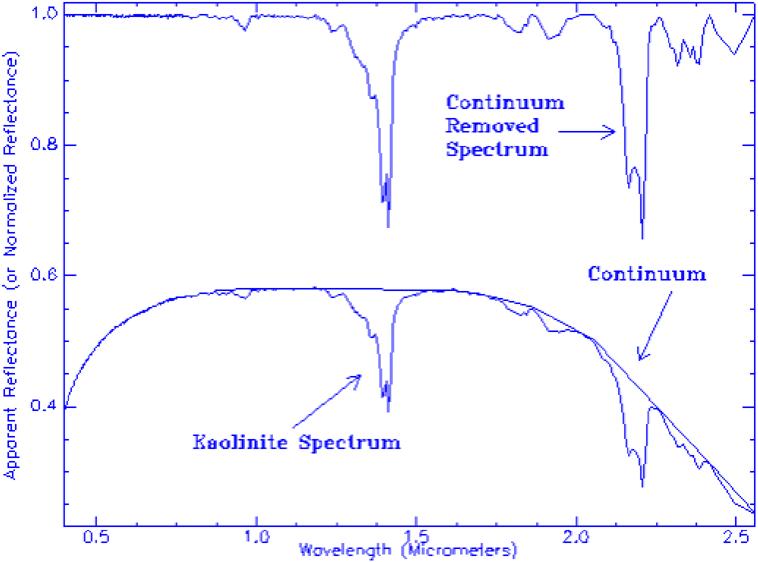

METHODS: Spectral Angle Mapper (SAM) Classifier

- SAM – pixel based supervised classification technique
- Measures the similarity of an image pixel reflectance spectrum to a reference spectrum
- Spectral angle (in radians) between the two spectra

$$\theta(\vec{\mathbf{x}}) = \cos^{-1}\left(\frac{f(\lambda)\cdot e(\lambda)}{||f(\lambda)||\cdot||e(\lambda)||}\right), \quad (1)$$

  $f(\lambda)$ – image reflectance spectrum and $e(\lambda)$ – reference spectrum.

- Results in a gray-scale rule image – values are the angles

METHODS (cont. . .): Spectral Angle Mapper (SAM) Classifier

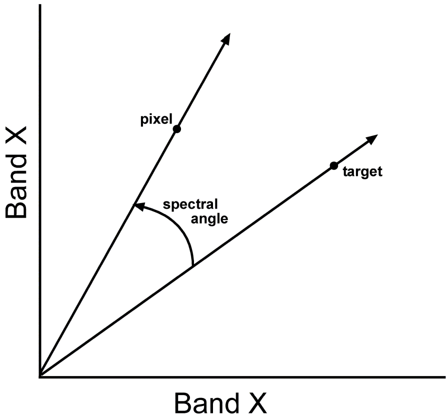

Figure: Spectral angle.

METHODS (cont. . .): SAM Rule Image for Alunite

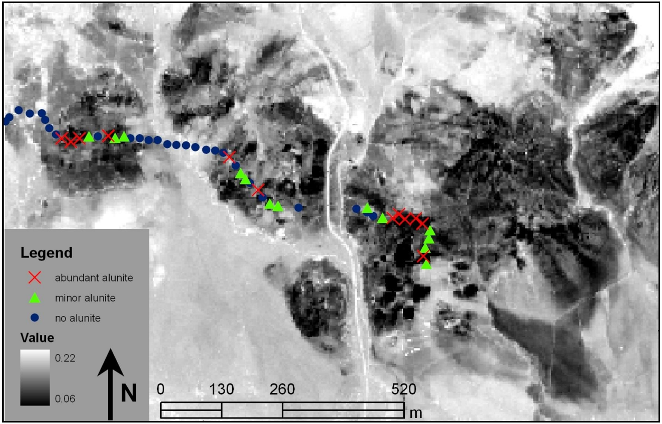

Figure: SAM classification rule image for alunite. Dark areas indicate smaller angles, hence, greater similarity to alunite.

METHODS (cont. . .): Spectral Feature Fitting (SFF)

- SFF – pixel based supervised classification technique
- Measures the similarity by examining specific absorption features in the spectrum after continuum removal has been applied to both the image and reference spectrum
- Performs a least squares fit on the absorption feature
- Results in a gray-scale rule image – values in the image are the fit

METHODS (cont. . .): SFF Rule Image for Alunite

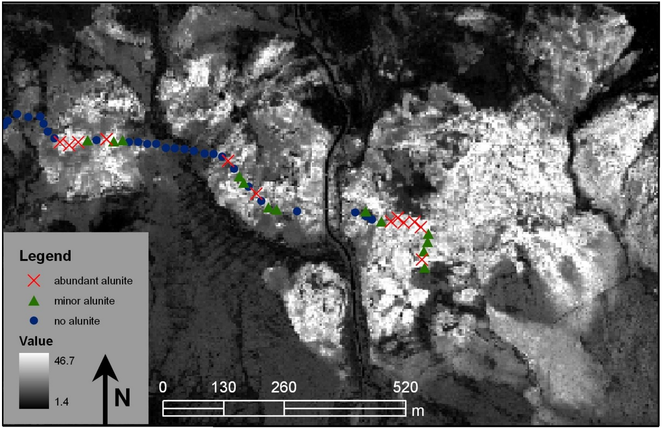

Figure: SFF fit image for alunite. Lighter areas indicate better fit values between pixel reflectance spectra and the alunite reference spectrum.

Using Remote Sensing Images to Design Optimal Field Sampling Schemes

Debba

Introduction

Optimized sampling schemes case studies

Optimized field sampling representing the overall distribution of a particular mineral

Deriving optimal exploration target zones

Combination of SAM and SFF scaled to $[0,1]$ is defined as

$$w(\theta(\vec{\mathbf{x}}), \tau_F(\vec{\mathbf{x}})) = \begin{cases} \kappa_1 w_1(\theta(\vec{\mathbf{x}})) + \kappa_2 w_2(\tau_F(\vec{\mathbf{x}})) \,, & \\ \qquad \text{if } \theta(\vec{\mathbf{x}}) \leq \theta^t \text{ and } \tau_F(\vec{\mathbf{x}}) \geq \tau_F^t & \\ 0 \,, \quad \text{if otherwise} & \end{cases} \tag{2}$$

$$\phi_{\text{WMSD}}(\mathbf{S}^n) = \frac{1}{N} \sum_{\vec{\mathbf{x}} \in \mathbf{I}} w(\vec{\mathbf{x}}) \, \left|\left| \vec{\mathbf{x}} - W_{\mathbf{S}^n}(\vec{\mathbf{x}}) \right|\right| \,, \tag{3}$$

METHODS (cont. . .): Fitness Function

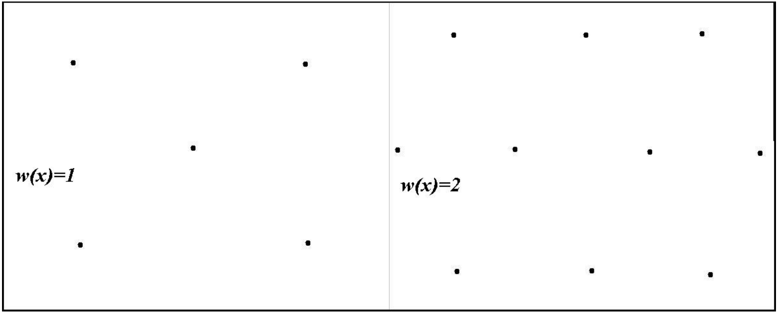

Figure: Fitness function with different weights for $N = 15$.

RESULTS (cont...): OPTIMIZED SAMPLING SCHEME

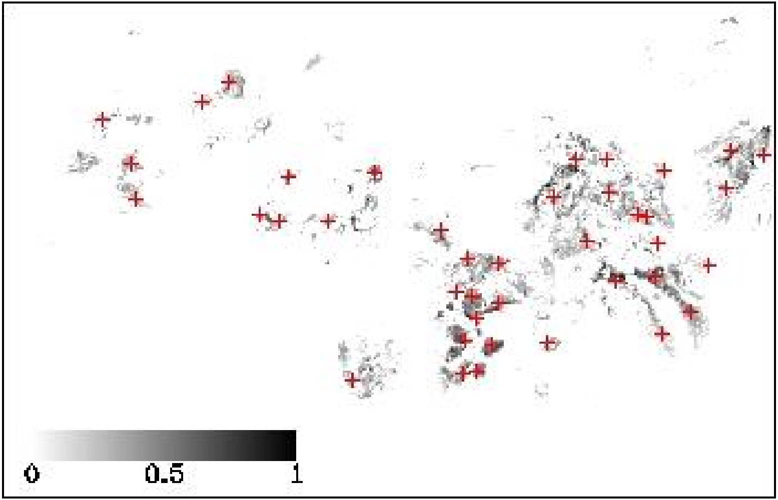

Figure: Optimized sampling scheme.

RESULTS (cont. . .): Distribution of 40 highest values

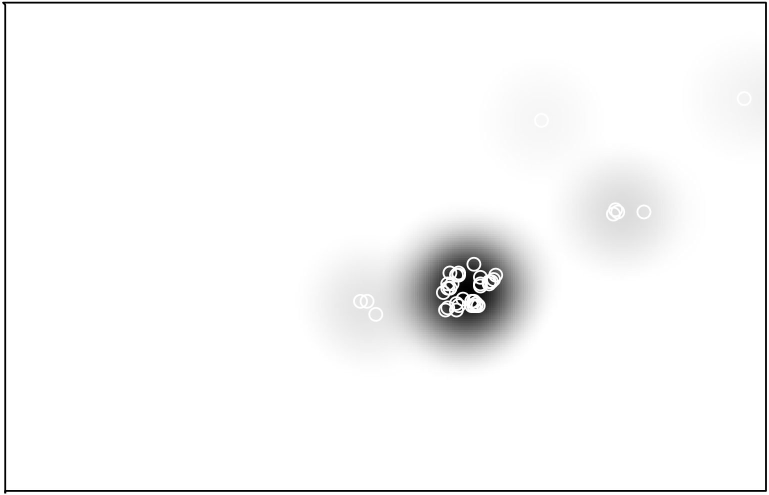

Figure: Sampling scheme: 40 highest values

RESULTS (cont. . .): Distribution of 40 optimized sampling scheme

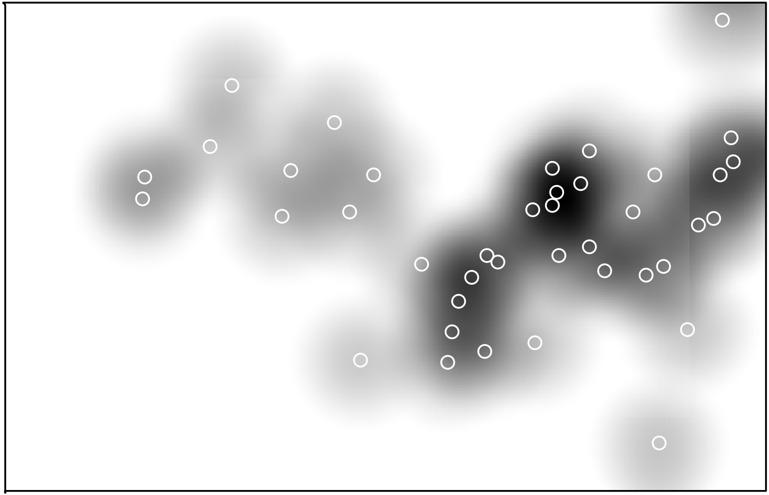

Figure: Distribution of 40 optimized sampling scheme

Outline

BACKGROUND AND OBJECTIVE OF STUDY

The location of known mineral occurrences (mines/prospects) are used for training in data-driven predictive mapping of prospective ground. Particular methods for obtaining a mineral prospective map are

- the weights-of-evidence (WofE) method
- logistic regression
- canonical favorability analysis
- neural networks
- evidential belief functions

BACKGROUND AND OBJECTIVE OF STUDY (cont. . .)

Mineral prospectivity maps are then usually used to guide further mineral exploration. A logical question regarding efficacy of mineral prospectivity maps is: "Where should targets of exploration for undiscovered mineral occurrences be focussed?"

The objective of this study is to demonstrate a methodology that we have developed in order to provide a plausible answer to the above question in a district-scale case study.

STUDY SITE

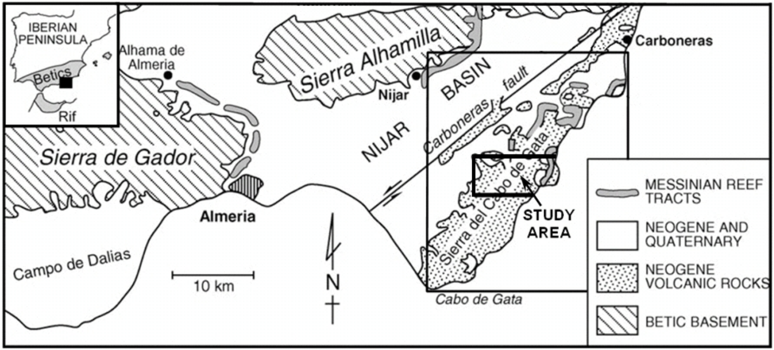

Figure: A generalized geological map of the Rodalquilar area mineral district.

DATA USED

- Two sets of locations of mineral deposit occurrences, from different sources, were used in WofE modeling.
- Set 1: 14 epithermal deposits and set 2: 36 epithermal deposits.
- Set 2: Training set for WofE and designing optimal exploration target zones.
- Set 1: Validation of WofE and optimal exploration target zones.
- HyMap: 126 bands – 0.4–2.5 μm
- Geology: 30 bands – 1.95–2.48 μm
- Distinctive absorption features at wavelengths near 2.2 μm

DATA USED (cont. . .): CREATION OF BAND RATIO AS EVIDENCES

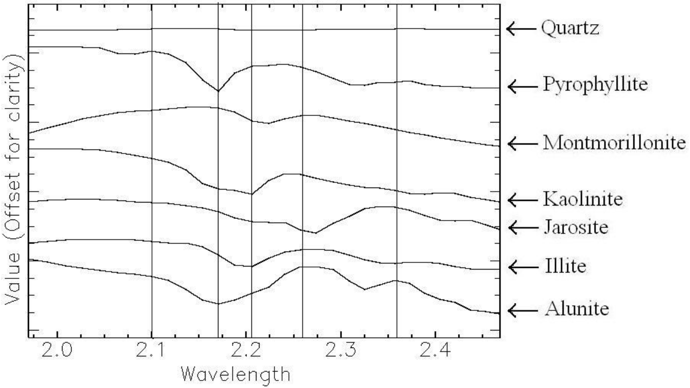

Figure: Plot of seven endmembers from USGS spectral library in the spectral range 1.95–2.48 μm. Vertical lines indicate the band centers used to obtain band ratio images (see text for further information).

DATA USED (cont. . .): CREATION OF BAND RATIO AS EVIDENCES

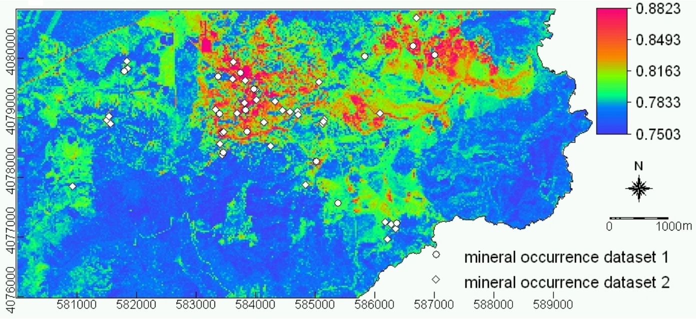

Figure: Band Ratio 1: arctan transformation on bands 103/107 (2.100/2.171 μm).

DATA USED (cont. . .): CREATION OF BAND RATIO AS EVIDENCES

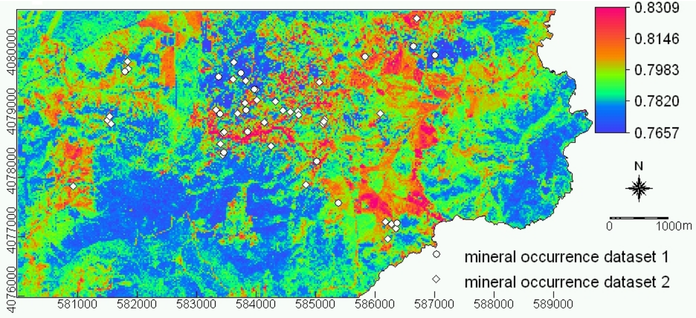

Figure: Band Ratio 2: arctan transformation on bands 107/109 (2.171/2.205 μm).

DATA USED (cont. . .): CREATION OF BAND RATIO AS EVIDENCES

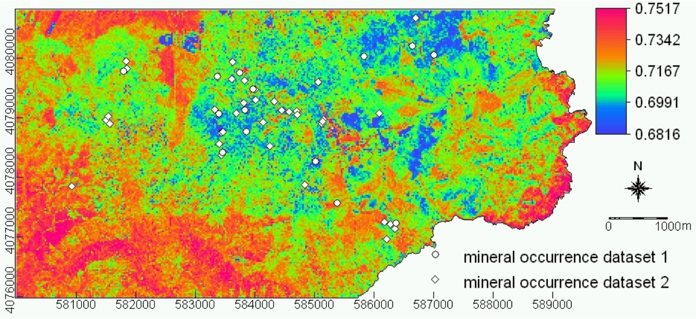

Figure: Band Ratio 3: arctan transformation on bands 118/112 (2.357/2.258 μm).

DATA USED (cont. . .): CREATION OF STRUCTURAL EVIDENCE

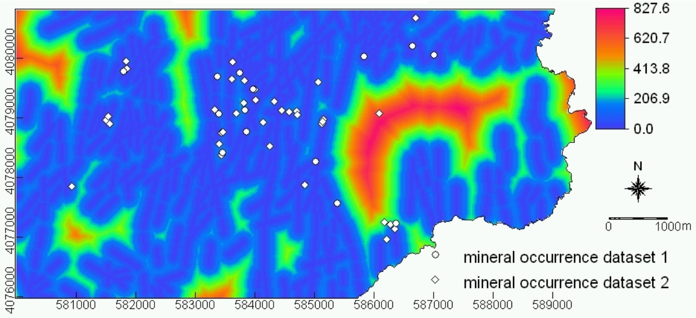

Figure: Distance to fault and fracture. Increasing pixel brightness in this image indicates increasing distance from a fault or fracture.

METHODS

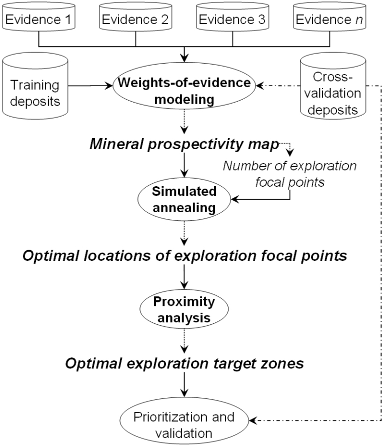

Figure: Flow diagram describing the process.

METHODS (cont. . .): ESTIMATION OF THE NUMBER OF EXPLORATION FOCAL POINTS

To estimate the number of exploration focal points, we used the binomial distribution – mineral deposit occurrence is a binary variable, being either present or absent.
Thus, estimation of n exploration focal points so as to yield (or discover) at least r mineral deposit occurrences, with a probability of success p, at a 95% confidence, requires a solution for the following equation:

$$\sum_{i=r}^{n} \binom{n}{i} p^i (1-p)^{n-i} = 0.95 \,. \tag{4}$$

METHODS (cont. . .): FITNESS FUNCTION

$$\phi_{\mathrm{WMSD+V}}(\mathbf{S}^n) = \frac{\lambda}{N(A)} \sum_{\vec{\mathbf{x}} \in A} P(\vec{\mathbf{x}}) \left|\left|\vec{\mathbf{x}} - Q_{\mathbf{S}^n}(\vec{\mathbf{x}})\right|\right| + (1-\lambda)s^2(O_{\mathbf{S}^n}) \,, \qquad (5)$$

where $Q_{\mathbf{S}^n}(\vec{\mathbf{x}})$ is the location vector of an optimal exploration focal point in $\mathbf{S}^n$ nearest to $\vec{\mathbf{x}}$, and $s^2(O_{\mathbf{S}^n})$ is the variance of the posterior odds.

RESULTS: ESTIMATION OF THE NUMBER OF EXPLORATION FOCAL POINTS

Assume

- $r = 9$ based on the nine predicted out of 14 undiscovered epithermal occurrences in training set 1
- $p = 0.0025$ based on the average posterior probabilities of prospective pixels in the input WofE prospectivity model

With these assumptions we derive $n = 6280$.
Instead of $p = 0.0025$, we used $p = 0.6$ based on the approximate prediction rate of the input WofE model.
Accordingly, $n = 22$

Using Remote Sensing Images to Design Optimal Field Sampling Schemes

Debba

Introduction

Optimized sampling schemes case studies

Optimized field sampling representing the overall distribution of a particular mineral

Deriving optimal exploration target zones

RESULTS (cont. . .): OPTIMIZED TARGET ZONES

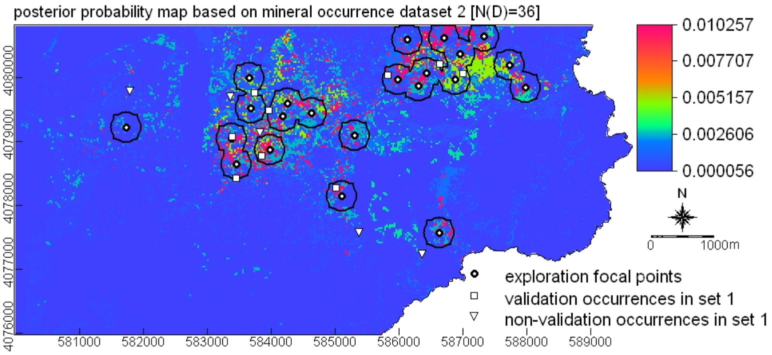

Figure: Optimal exploration target zones defined by buffering to 238 m each of the optimal exploration focal points.

RESULTS (cont. . .): OPTIMIZED TARGET ZONES

- Total area represented by the 6280 unit cells is approximately $6280 \times 25^2 = 3925000\,\text{m}^2$.
- Delineated sub-area of $3925000/22 = 178409\,\text{m}^2$
- If assumed undiscovered deposit is within a radius of $\sqrt{178409/\pi} = 238\,\text{m}$ (area of circle $= \pi \times \text{radius}^2$) around a derived optimal exploration focal point – then close.